Physical Exercise–Induced Hypoglycemia Caused by Failed Silencing of Monocarboxylate Transporter 1 in Pancreatic β Cells

Timo Otonkoski, Hong Jiao, Nina Kaminen-Ahola, Isabel Tapia-Paez, Mohammed S. Ullah, Laura E. Parton, Frans Schuit, Roel Quintens, Ilkka Sipilä, Ertan Mayatepek, Thomas Meissner, Andrew P. Halestrap, Guy A. Rutter, and Juha Kere

Exercise-induced hyperinsulinism (EIHI) is a dominantly inherited hypoglycemic disorder characterized by inappropriate insulin secretion during anaerobic exercise or on pyruvate load. We aimed to identify the molecular basis of this novel disorder of β-cell regulation. EIHI mapped to chromosome 1 (LOD score 3.6) in a genome scan performed for two families with 10 EIHI-affected patients. Mutational analysis of the promoter of the *SLC16A1* gene, which encodes monocarboxylate transporter 1 (MCT1), located under the linkage peak, revealed changes in all 13 identified patients with EIHI. Patient fibroblasts displayed abnormally high *SLC16A1* transcript levels, although monocarboxylate transport activities were not changed in these cells, reflecting additional posttranscriptional control of MCT1 levels in extrapancreatic tissues. By contrast, when examined in β cells, either of two *SLC16A1* mutations identified in separate pedigrees resulted in increased protein binding to the corresponding promoter elements and marked (3- or 10-fold) transcriptional stimulation of *SLC16A1* promoter-reporter constructs. These studies show that promoter-activating mutations in EIHI induce *SLC16A1* expression in β cells, where this gene is not usually transcribed, permitting pyruvate uptake and pyruvate-stimulated insulin release despite ensuing hypoglycemia. These findings describe a novel disease mechanism based on the failure of cell-specific transcriptional silencing of a gene that is highly expressed in other tissues.

Release of insulin from the pancreatic β cell is carefully controlled by metabolic demands, allowing maintenance of the circulating blood-glucose concentration within narrow physiological limits. It is therefore important that insulin release be strongly stimulated as glucose concentrations rise but also effectively switched off during fasting, to avoid hypoglycemia.[1] β-cell metabolism has specific features to ensure the latter. First, β cells express the low-affinity glucose transporter GLUT2[2] and glucose phosphorylating activity, glucokinase,[3] to permit enhanced glucose metabolism as the concentration of the sugar changes over the physiological range.[1] Second, the activity of lactate dehydrogenase is unusually low.[4–6] Third, the expression of the plasma-membrane monocarboxylate transporter (MCT) MCT1 (*SLC16A1* [MIM 600682]) as well as of other MCT isoforms[7] is weak or undetectable in the β cell.[8] This configuration has been proposed to reduce loss-of-glucose carbon as pyruvate [6] and to avoid the unwanted stimulation of insulin release by lactate or pyruvate.[9]

We recently identified exercise-induced hyperinsulinism (EIHI) as a dominantly inherited hypoglycemic disorder characterized by inappropriate insulin secretion, particularly during anaerobic exercise.[10–12] Affected patients become hypoglycemic within 30 min after a short period of anaerobic exercise. This pathology might result from an inappropriate insulin release in response to exogenous catabolic metabolites such as lactate and pyruvate. Indeed, unlike unaffected individuals, patients responded to an acute exogenous pyruvate load with prompt insulin release.[11] This could be due to an overactivity of MCTs in the β-cell plasma membrane, which leads to the entry of pyruvate into the cell followed by its metabolism with a consequent increase in ATP production and insulin secretion. However, in earlier studies, no mutations were detected in the coding regions of eight MCT genes.[11] Therefore, we decided to map the disease gene, to identify the specific mutations, and to test their pathogenetic mechanisms in the β cell.

Material and Methods

Patients

Our study includes all 13 reported patients with EIHI. Twelve patients belong to two Finnish pedigrees. Their clinical phenotypes were described elsewhere.[11] However, DNA for linkage analysis was available from only 10 of the 12 (fig. 1). The fold response of insulin secretion to an intravenous bolus of sodium pyruvate provided the basis for differentiating affected and unaffected in-

From the Hospital for Children and Adolescents and Biomedicum Helsinki, Faculty of Medicine (T.O.; I.S.), and Department of Medical Genetics (N.K.-A.; J.K.), University of Helsinki, Helsinki; Department of Biosciences and Nutrition, Karolinska Institutet, Stockholm (H.J.; I.T.-P.; J.K.); Henry Wellcome Laboratories for Integrated Cell Signalling and Department of Biochemistry, School of Medical Sciences, University of Bristol, Bristol, United Kingdom (M.S.U.; L.E.P.; A.P.H.; G.A.R.); Department of Molecular Cell Biology, Katholieke Universiteit Leuven, Leuven, Belgium (F.S.; R.Q.); Department of General Pediatrics, University Children's Hospital, Düsseldorf (E.M.; T.M.); and Department of Cell Biology, Division of Medicine, Imperial College London, London (G.A.R.)

Received March 8, 2007; accepted for publication May 21, 2007; electronically published July 26, 2007.

Address for correspondence and reprints: Dr. Timo Otonkoski, Biomedicum Helsinki, Room C507b, P.O. Box 63, FIN-00014 University of Helsinki, Helsinki, Finland. E-mail: timo.otonkoski@helsinki.fi

Am. J. Hum. Genet. 2007;81:467–474. 0002-9297/2007/8103-0005$15.00
DOI: 10.1086/520960

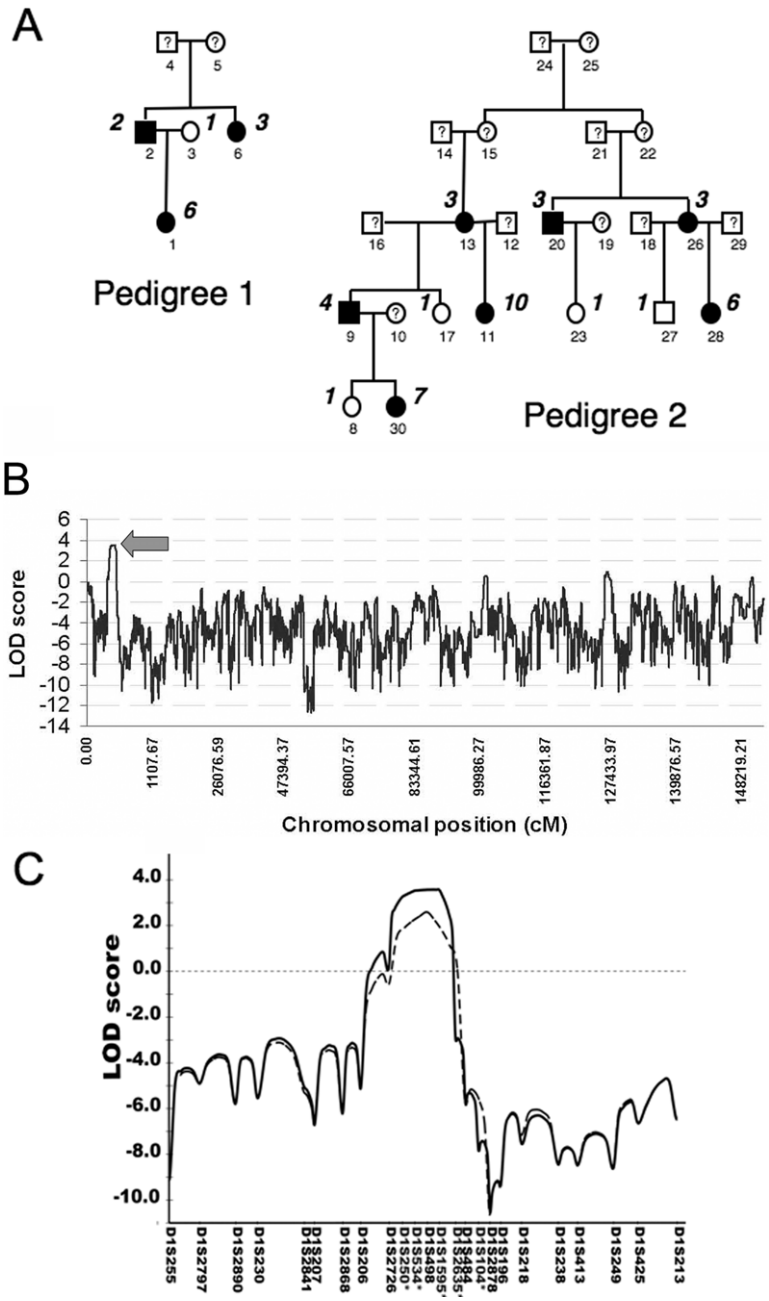

Figure 1. EIHI-affected families for genomewide linkage analysis and LOD scores on the chromosome 1 linkage region. *A,* EIHI-affected families. Ten affected individuals (1, 2, 6, 9, 11, 13, 20, 26, 28, and 30) and nine unaffected (3, 8, 16, 17, 18, 19, 22, 23, and 27) were genotyped and used for linkage analysis. The fold response of insulin secretion in response to pyruvate challenge is indicated in italics above the symbol representing subjects tested, as a definitive phenotypic feature differentiating affected and unaffected individuals. *B,* Parametric LOD-score curve from genomewide linkage analysis of 435 microsatellite markers with use of a dominant model of inheritance. The only genomewide-significant peak is near the centromere of chromosome 1p (*arrow*). *C,* Higher resolution LOD-score curve at the linkage peak on chromosome 1p. The dashed line represents the initial linkage analysis, and the solid line shows fine-mapping with five additional markers (marked with asterisks [*]).

dividuals. In all the unaffected individuals, this fold response has a value of 1; in the affected individuals, it has a range of 2–10 (fig. 1*A*).[11] One patient is from Germany; the pathophysiology of his insulin secretion during physical exercise has been studied in detail.[12]

Genetic Linkage Analysis

Genomic DNA was extracted from whole blood (PureGene [Gentra Systems]). A genomewide scan was performed with 430 microsatellite markers from the Linkage Mapping Set MD-10 (Ap-

plied Biosystems) on a MegaBace 1000 capillary sequencer (Molecular Dynamics). The alleles were visualized using Genetic Profiler 1.1 or 2.0 software (Molecular Dynamics). For fine mapping, five microsatellites were added to the highest peak region. Genotyping was performed at the Finnish Genome Center (genome scan) and Clinical Research Center, Karolinska Institutet (fine mapping). Parametric linkage analysis with use of GENEHUNTER (v. 2.1)[13] was based on an autosomal dominant model with a penetrance of 0.999 for heterozygotes, disease-allele frequency of 0.001, and phenocopy rate of 0.001. The positions of marker loci were based on published maps (National Center for Biotechnology Information [NCBI]).

Sequencing the Candidate Genes

One patient sample from both families and a control sample were sequenced in both directions for the 5′ and 3′ UTRs and 2-kb promoter region of the MCT1 gene (*SLC16A1*) and all exons and 1 kb of the promoter of the *HMGCS2* gene. The primer sequences are available on request. Purified (PCR purification kit and gel-extraction kit [Qiagen]) PCR products were sequenced using ABI 377 or ABI 3100 (Applied Biosystems). The Staden package[14] was employed for sequence alignment and comparison. Sequences were checked against the published genome (NCBI). To verify the frequency of the sequence changes in healthy individuals, 94 control samples from Finland and 32 control samples from Germany were sequenced.

Quantitative RT-PCR Analysis of MCT1 mRNA Expression

Tissues were from male C57BL/6 mice (aged 8–10 wks). Islets of Langerhans and pancreatic acini were collagenase isolated (for 3 min at 37°C) and were hand picked under a dissection microscope.[15] Embryonic stem (ES) cells were obtained from L. Schoonjans (Thrombix, Center of Vascular Biology, Katholieke Universiteit). MIN6 cells were obtained from E. Yamato (Division of Stem Cell Regulation Research, Osaka University Medical School). Total RNA from tissues was isolated using TRIzol (Invitrogen) followed by cleanup with RNeasy (Qiagen). Total RNA from islets, acini, ES cells, and MIN6 cells was extracted using the Absolutely RNA microprep kit (Stratagene). RNA quality and quantity were assessed using the 2100 BioAnalyzer (Agilent Technologies) and the NanoDrop ND-1000 spectrophotometer. One microgram of total RNA was used for cDNA synthesis with the RevertAid H Minus M-MuLV Reverse Transcriptase kit (Fermentas). Quantitative PCRs (qPCRs) were performed using ABsolute QPCR mix (ABgene) on a Rotor-Gene 3000 (Corbett Research). Quantification of *MCT1* mRNA-expression levels was normalized using polymerase II alpha (Polr2a) mRNA as internal reference. In each run, a MIN6 cell sample was used as a calibrator, and relative *MCT1* mRNA expression for this sample was set at 1.0. Reaction conditions and sequences for primers and dual-labeled fluorescent probes, synthesized by Sigma Genosys, are available on request. Significance of differences in mRNA expression was assessed using the two-tailed unpaired Student's *t*-test. Standard curves were constructed by amplifying serial dilutions of untreated mhAT3F cDNA (50 ng to 0.64 pg) and by plotting cycle threshold (C_T) values as a function of starting reverse-transcribed RNA, the slope of which was used to calculate relative expression of the target gene.[16]

MCT1 Promoter Cloning and Site-Directed Mutagenesis

Bases from −1342 to +216A in the *MCT1* promoter[17] were amplified using primers 5′-ACT GTC TTC TAA TAT ACT GAA CTG TTA TTG G-3′ and 5′-TCG TTT GCT TGT TCC AGT ACC CAC GCA-3′. PCR was performed using genomic DNA as template. The single 1.5-kb band was gel extracted and cloned into the pGEM T-Easy vector (Promega). The promoter fragment was then excised by digestion with *Eco*RI and was subcloned into the CFP-N vector. *Hin*dIII and *Kpn*I digestion of the resulting construct produced a 1,558-bp *MCT1* promoter fragment, which was ligated into pGL3-Basic vector (Promega).

A point mutation was introduced at position +163 of the *MCT1* promoter, with use of the QuickChange kit (Stratagene). A 1,595-bp MCT1 promoter region containing the 25-nt duplication was cloned using patient fibroblast–derived genomic DNA, with use of primers 5′-GGATGCCACACTGTCTTCTAATA-3′ and 5′- CCTC-GTTTGCTTGTTCCAGTA-3′. The presence of the desired mutations was confirmed by sequencing.

MCT1 Promoter Assay

MIN6 β cells were seeded in a 24-well plate at a density of 2×10^5 ml^{-1} and were cotransfected for 4 h with 800 ng pGL3-promoter vector containing either wild-type or mutant hSLC16A1 promoter sequences, as detailed above, with 100 ng pRL-SV40 (Promega) containing *Rotylenchulus reniformis* luciferase gene as a control for transfection efficiency, with 10 μg ml^{-1} Lipofectamine in Opti-MEM I medium (Invitrogen). Cells were harvested 48 h after transfection and were assayed for luciferase activity with the Dual-Glow Luciferase Assay System (Promega). Promoter activities were expressed as relative light units normalized against control reporter (*R. reniformis* luciferase) activity in each extract, as described elsewhere.[18]

Electrophoretic Mobility Shift Assay (EMSA)

EMSA was performed according to standard protocols.[19] In brief, 10-μg aliquots of MIN-6 nuclear extracts were preincubated with 0.5 μg of poly (dI-dC) and 1 μl of 100 mM dithiothreitol (DTT) in a 30-μl reaction with a 4 × buffer—containing 80 mM HEPES (pH 7.6), 2 mM EDTA, 200 mM NaCl, 20% glycerol, 1.2 mg BSA, and 40 mM DTT—for 15 min at room temperature. ^{32}P-end–labeled double-stranded wild-type or mutant probes were added, and the mixture was incubated for 15 min at room temperature. In competition assays, cold probes were incubated with 100- and 200-molar excess for 15 min at room temperature before the addition of the labeled probes. The samples were electrophoresed on 4.5% nondenaturing polyacrylamide gels in 1 × TBE at 240 V in a cold room. The radioactive pattern was visualized by autoradiography and was quantified by PhosphorImager scanning (Fuji Photo). Oligonucleotides were normal probes (5′-GCC CGG CCA GAC AAA ***G***TG GTG AGC TGC GAC-3′ and 5′-GTC GCA GCT CAC CA***C*** TTT GTC TGG CCG GGC-3′) and mutant probes (5′-GCC CGG CCA GAC AAA ***A***TG GTG AGC TGC GAC-3′ and 5′-GTC GCA GCT CAC CA***T*** TTT GTC TGG CCG GGC-3′).

Experiments with Patient Fibroblasts

Primary fibroblast cell lines were generated from skin-biopsy samples of one patient from each family and from four healthy age-matched control individuals. Steady-state levels of MCT1 and MCT4 protein and mRNA were measured by western blotting[18]

and quantitative RT-PCR, respectively. Total RNA was isolated from cultured fibroblasts (TRI Reagent [Sigma]) and was DNAse treated (DNA-free [Ambion]) as recommended by the supplier. First-strand cDNA was synthesized from 2 μg total RNA. TaqMan primers and probes for quantitative RT-PCR were kindly donated by AstraZeneca (R&D Charnwood). The dual-labeled fluorogenic probes consisted of oligonucleotides with the 5′ reporter dye 6-carboxyfluorescein (FAM) and the 3′ Black Hole Quencher 1 dye (BHQ1). Primer and probe sequences are available on request. Lactate transport into the fibroblasts was determined by measurement of the decrease in intracellular pH with use of the fluorescent pH-sensitive dye 2′–7′-bis (carboxyethyl)-5–6-carboxyfluorescein (BCECF) as described elsewhere.[20]

Results

Identification of SLC16A1 *Mutations*

We diagnosed EIHI for 13 patients, 12 from two families and one unrelated patient. A total of 430 microsatellite markers were genotyped in 10 affected and 9 unaffected individuals (fig. 1*A*). Linkage analysis with a dominant model revealed the strongest evidence of linkage on chromosome 1, with total maximum LOD score 2.53 (fig. 1*B*). Five markers were added to the linkage peak, with an increase of maximum LOD score to 3.6 (fig. 1*C*). Four adjacent markers showed significant linkage by single-point analysis. A haplotype formed by markers *D1S250, D1S534, D1S498,* and *D1S1595* was present in all affected but no unaffected individuals of the larger family. Nor was it present in the other pedigree, suggesting that the families have independent mutations.

Several candidate genes with potential relevance were present within the linkage peak. We initially elected three of them for sequencing. The *PHGDH* gene, which encodes phosphoglycerate dehydrogenase (MIM 606879), was located 580 kb from peak marker *D1S534.* The *HMGCS2* gene, which encodes mitochondrial 3-hydroxy-3-methylglutaryl-coenzyme A synthase 2 (MIM 600234) was 620 kb from *D1S534,* and the *SLC16A1* gene, which encodes the MCT1 protein (MIM 600682), was located 6.2 Mb from the peak marker. We sequenced all three genes; no sequence variants were found in any exons of *HMGCS2,* but two variants in *PHGDH—rs562038* and *rs543703* in exon 1 and exon 11, respectively—were found in the EIHI-affected families. Sequencing of *SLC16A1* was focused on the 5′ UTR and promoter regions (2 kb upstream of the transcription start site) because no mutations had been found previously in the coding region.[11] A previously unknown SNP (a G→A change) in exon 1 at position +163 relative to the transcription start site, was found in the affected individuals of pedigree 1 (fig. 2*A*). In a patient from pedigree 2, a 25-bp duplication was found between nucleotide positions −23 and −24. The duplicated sequence also contained an A→T change (fig. 2*A* and 2*C*). Sequencing of these putative mutations in at least 94 samples from Finland and Germany revealed not a single occurrence in healthy controls, excluding with >84% probability that they were polymorphisms with a frequency of $\geq$1%. In the German patient,[10,12] several sequence variants were found, including a 2-bp insertion (fig. 2*B*).

Database searching (TESS: Transcription Element Search System) revealed that the three putative mutations lie within the binding sites of several transcription factors (fig. 2*A* and 2*B*). A binding site for nuclear matrix protein 1 (YY1) was predicted at the point-mutation site in the mutant sequence of pedigree 1. The same point mutation disrupted the binding sites of two potential transcriptional repressors: albumin negative factor (ANF) and AML-1a (fig. 2*A*). The duplication variant introduced additional binding sites for the ubiquitous transcription factors simian-virus-40-protein-1 (Sp1), upstream stimulatory factor (USF), and myeloid zinc finger 1 (MZF1) (fig. 2*A*). The third mutation resulted in loss of a GATA-1–binding site (fig. 2*B*). These predictions were consistent with the hypothesis that the identified mutations affect regulation of the *SLC16A1* gene.

Functional Consequences of the Mutations

To establish potential functional consequences of the +163 G→A variant in pedigree 1, we performed EMSA. Distinct differences were seen in the protein-binding activity of this site in nuclear extracts, with binding to the common variant increasing progressively in MIN6, SyH-SY5Y, and HeLa cells (fig. 3). Moreover, in each cell type, a higher degree of binding to the mutated site was apparent, except for one low–molecular weight band that was lost in the mutated sequence in MIN6 cells (fig. 3). Competition assays confirmed the specificity of the probes. The EMSA result provided further evidence of altered transcriptional regulation introduced by the G→A mutation.

Since it was not feasible to study *SLC16A1* promoter activity in patient β cells, mRNA expression in skin fibroblasts from two EIHI-affected patients and four control individuals was assayed for two genes, *SLC16A1* (which encode MCT1) and *SLC16A3* (which encodes MCT4). As measured by quantitative RT-PCR (normalized against 18S RNA), MCT1 mRNA was two to three times higher in both patients than it was in any control, whereas MCT4 mRNA levels were similar in patients and controls. To determine whether the increase in *SLC16A1* mRNA in patient fibroblasts led to increased expression of MCT1 and monocarboxylate transport activity, western blotting and transport assays were performed (fig. 4). There was no evidence that the patient fibroblasts showed greater expression or activity than did the control fibroblasts. This lack of correlation between levels of MCT1 mRNA and MCT1 protein is well established in a variety of tissues and is thought to result from posttranscriptional regulation involving the unusually long (1.6 kb) 3′ UTR of MCT1 mRNA.[21,22] In most tissues, such as fibroblasts, the expression of MCT1 protein may be relatively insensitive to the level of MCT1 mRNA, which is controlled to a much greater extent by translational mechanisms. However, in the β cell, where the basal

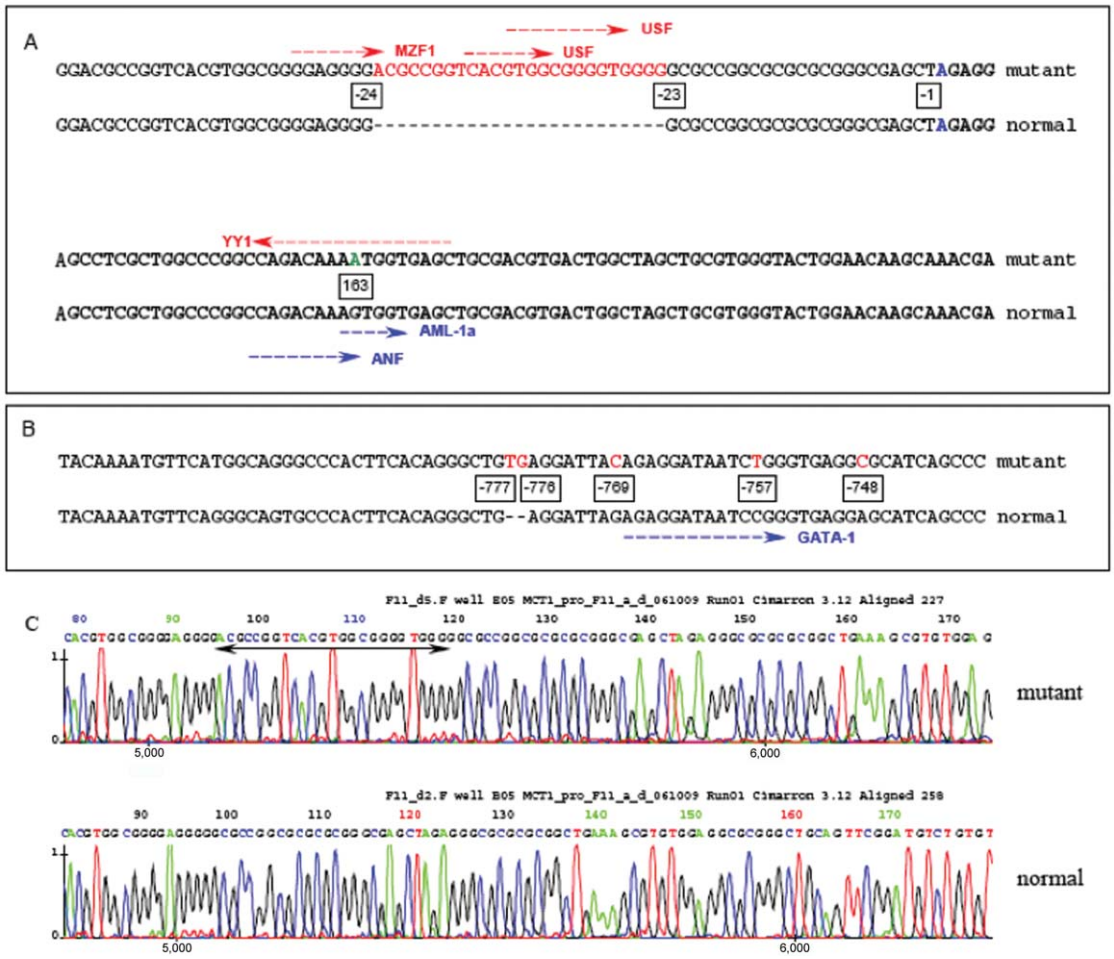

Figure 2. Alignment of nucleotide sequence of the 5′ region of the normal and mutated MCT1 gene. The noncoding exon 1 is shown in bold black font, and the transcription start site is indicated in blue. Numbers in boxes indicate nucleotide positions. *A,* Mutations found in Finnish families. A SNP in exon 1 at position 163, found in pedigree 1, is shown in green, and the duplicated sequence of pedigree 2 is shown in red. *B,* Mutation found in a German patient. Specific binding sites of transcription factors are indicated with arrows, red for gain in mutant and blue for loss in mutant. *C,* Sequences at the duplication site from a heterozygous patient of pedigree 2. The arrow bar indicates the duplicated sequence in one of two homologous chromosomes.

expression of MCT1 mRNA is extremely low, MCT1 protein expression may respond significantly to the increased mRNA production that results from the activated promoter in the patients.

The potential functional relevance of the above findings for β cells was tested by measuring MCT1 mRNA levels in a number of mouse tissues, including purified pancreatic acini and islets, clonal murine β cells (MIN6), and α cells (αTC1-9) (fig. 5*A* and 5*B*). Compared with all other tissues, MCT1 mRNA was very low or absent in β cells and islets, consistent with differences reported elsewhere in lactate-transport activity[4] and MCT1 levels[8] in pancreatic β cells. Transfection of MIN6 cells with an MCT1 promoter-luciferase reporter construct including the nucleotides from -1342 to $+216$ revealed a 3.5-fold ($P < .001$) increase in promoter activity after the G→A mutation at position 163 (fig. 5*C,* mutation P1). A similar (two-to-threefold) increase in the MCT1 promoter activity induced by this mutation was seen when the same promoter-luciferase reporter constructs were expressed in L6 myoblasts and HeLa and CHO cells (data not shown). Transfection of the MIN-6 cells with a promoter construct, including the 25-nt duplication found in pedigree 2, resulted in an even more dramatic (10-fold, $P < .001$) stimulatory effect on transcription (fig. 5*C,* mutation P2).

Discussion

We identify here linkage to mutations in the *SLC16A1* gene in two pedigrees of patients with EIHI. Whereas the linkage interval was relatively large, we failed to detect mutations in other likely potential genes in this region, but we demonstrated instead that two of the three *SLC16A1* gene mutations lead to profound increases in

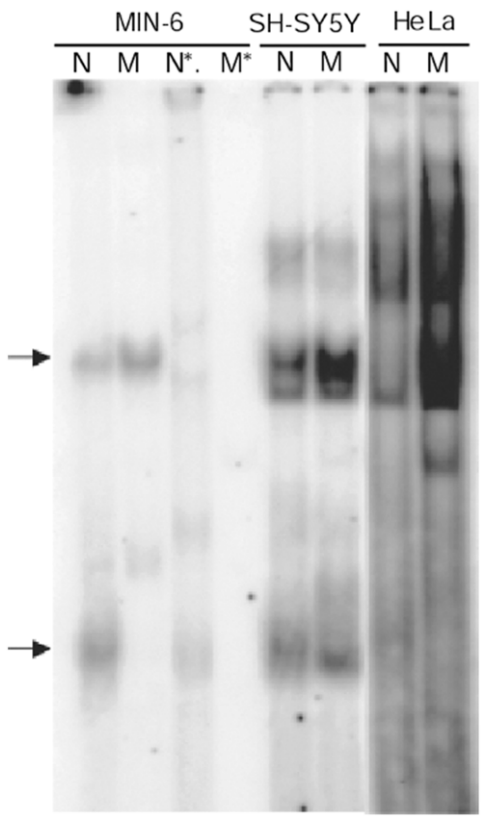

Figure 3. EMSAs performed using 30-bp fragments encompassing the polymorphism +163 G→A found in exon 1 of the *SLC16A1* gene. Protein extracts from three different cell lines were used: lanes 1–4, MIN-6 cells; lanes 5–6, SH-SY5Y cells; and lanes 7–8, HeLa cells. N denotes normal probe "G," and M denotes mutant probe "A." Lanes with asterisks (*) denote competition assays with unlabeled variants of the probe. Arrows indicate the differential affinity in the binding (*upper arrow*) and disruption of a putative binding site (*lower arrow*).

the transcription of this gene. These changes are likely to lead to increased levels of MCT1 protein, and hence transport activity, selectively in β cells where, in healthy subjects, MCT1 levels are extremely low. The present study thus suggests that human β cells, like those of rodents,[4,8] may be uniquely configured in this way. Low levels of plasma-membrane–lactate transport activity ensure that the uptake of lactate and pyruvate—and hence the inappropriate, and potentially fatal, secretion of insulin—does not occur during exercise. In patients with EIHI, selective increases in β-cell MCT1 expression may permit pyruvate or lactate to stimulate β-cell mitochondrial metabolism, leading to increased intracellular ATP/adenosine diphosphate ratios, the closure of K_{ATP} channels,[23] inhibition of adenosine monophosphate–activated protein kinase,[24] plasma membrane depolarization, Ca^{2+} influx, and insulin exocytosis.[1] Given the very low lactate dehydrogenase (LDH) activity in β cells,[6] the very efficient pyruvate oxidation by β-cell mitochondria,[23] and the fact that overexpression of both MCT1 and LDH was required for a secretory response to lactate in isolated islets,[9] we suspect that changes in circulating pyruvate, rather than lactate, are the principal trigger for insulin secretion in patients with EIHI.[11]

Our data are consistent with silencing of the MCT1 promoter in β cells by inhibitory transcription factors that remain to be characterized. Likewise, duplication of a *cis*-acting region, as seen in one pedigree, may provide increased basal transcriptional activity. In any case, the resulting increase in transcription, from near zero to a significant level, seems likely to lead to an increase in MCT1 activity in the β cell. Since our normal MCT1-promoter construct shows significant but low activity in MIN6 cells, additional posttranscriptional inhibitory

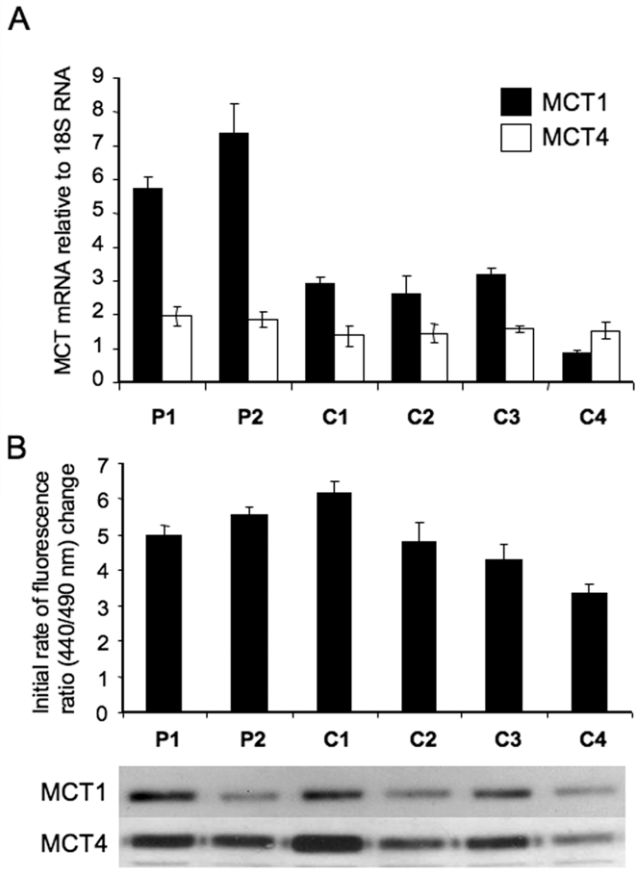

Figure 4. *A,* MCT1 and MCT4 mRNA expression in control and patient fibroblasts. Expression was normalized against ribosomal 18S expression. Data are the mean (±SEM) of four independent experiments, each involving triplicate measurements. *B,* Transport assay with use of pH-sensitive BCECF dye. Data are the mean (±SEM) of 8–14 individual cells per assay. *C,* Western-blot data showing MCT1 and MCT4 expression in cultured fibroblast cells. Whole-cell protein extracts were prepared from the same batch of cells that were assayed for lactate transport and were resolved using SDS-PAGE. Western blotting was performed with antibodies to MCT1 and MCT4, as indicated.

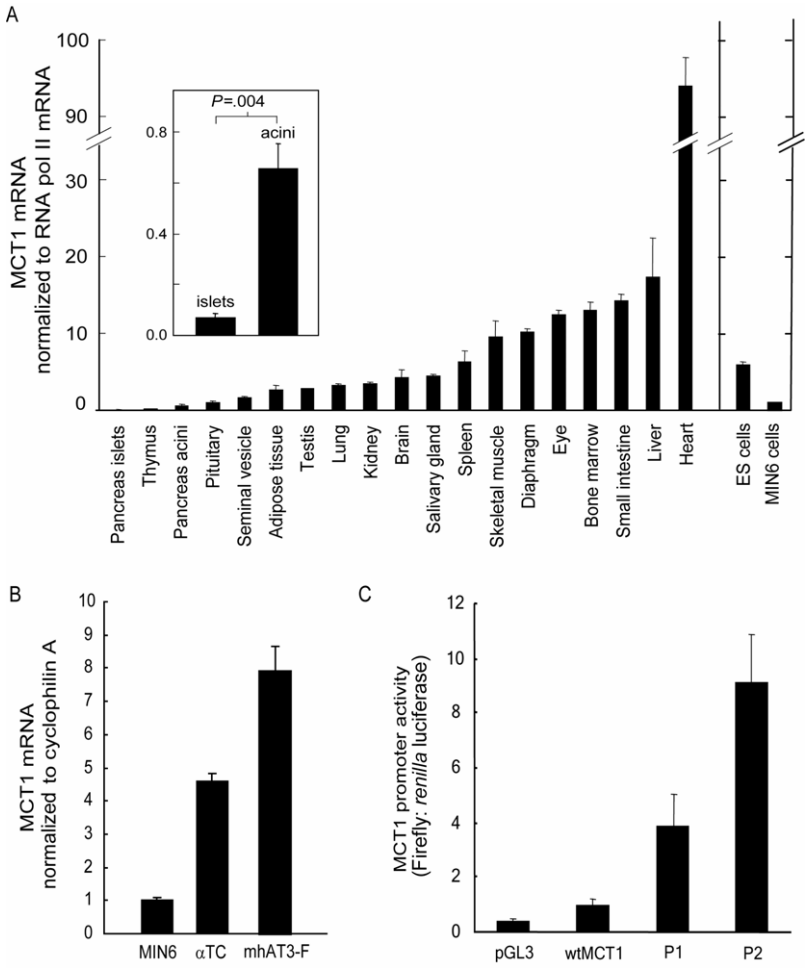

Figure 5. *A,* Ex vivo MCT1 mRNA expression in a panel of mouse tissues, including hand-picked pancreatic islets of Langerhans and pancreatic acini, as well as mouse ES cells and the insulin secreting cell line MIN6. MCT1 mRNA was quantified via quantitative RT-PCR and was normalized for RNA Polymerase II alpha (Polr2a). All PCR samples, including two MIN6 cell replicates, were calibrated against extract from a MIN6 cell that was scaled at a ratio of 1.0. Data are means (±SEM) of three independent biological replicates. The mouse tissues are ranked with increasing expression level. *Inset,* Pancreatic islets versus acini with an enlarged scale; significance of difference in the expression ratio was calculated with the unpaired two-tailed Students' *t*-test. *B,* Tissue-specific MCT1 mRNA expression. Real-time RT-PCR was performed on cDNA isolated from clonal pancreatic β cells (MIN6), α-cells (α-TC), hepatoma (mhAT3-F) as described in the "Material and Methods" section. Expression was normalized against cyclophilin, and results were expressed as fold change (±SEM) over MCT1 expression in MIN6. *C,* MCT1 promoter activity in MIN6 β cells. Activity was measured as the ratio of firefly:*renilla* luciferase activity after transfection with the control plasmid (pGL3), the wild-type promoter (wtMCT1), or the mutations found in the two pedigrees (P1 and P2). Data are presented as mean (±SEM) for six replicates in each case in three separate experiments.

mechanisms are likely to exist to further inhibit expression of MCT1 protein.

In conclusion, we describe here a novel mechanism for human disease. The failed silencing of the expression of a cell-membrane transporter (MCT1) in a specific cell type (pancreatic β cells) leads to an inappropriate physiological response in patients with EIHI, characterized by inappropriate insulin release during anaerobic exercise.

Acknowledgments

This study was supported by the Foundation for Pediatric Research (to T.O.), Academy of Finland and Sigrid Juselius Foundation (to J.K. and T.O.), Swedish Research Council (to J.K.), and Juvenile Diabetes Research Foundation (JDRFI) (to T.O. and F.S.). M.S.U. was supported by an Industrial Studentship from AstraZeneca (R&D Charnwood, Loughborough). G.A.R. thanks the Wellcome Trust for a Programme Grant and Research Leave Fellowship and thanks the National Institutes of Health, JDRFI, and Medical Research Council (UK).

Web Resources

The URLs for data presented herein are as follows:

Online Mendelian Inheritance in Man (OMIM), http://www.ncbi.nlm.nih.gov/Omim/ (for *SLC16A1,* phosphoglycerate dehy-

drogenase, 3-hydroxy-3-methylglutaryl-coenzyme A synthase 2, and MCT1 protein)

TESS: Transcription Element Search System, http://www.cbil.upenn.edu/cgi-bin/tess/tess

References

1. Rutter GA (2004) Visualising insulin secretion: the Minkowski Lecture 2004. Diabetologia 47:1861–1872
2. Thorens B, Sarkar HK, Kaback HR, Lodish HF (1988) Cloning and functional expression in bacteria of a novel glucose transporter present in liver, intestine, kidney, and β-pancreatic islet cells. Cell 55:281–290
3. Iynedjian PB (1993) Mammalian glucokinase and its gene. Biochem J 293:1–13
4. Sekine N, Cirulli V, Regazzi R, Brown LJ, Gine E, Tamarit-Rodriguez J, Girotti M, Marie S, MacDonald MJ, Wollheim CB, et al (1994) Low lactate dehydrogenase and high mitochondrial glycerol phosphate dehydrogenase in pancreatic beta-cells. Potential role in nutrient sensing. J Biol Chem 269: 4895–4902
5. Liang Y, Bai G, Doliba N, Buettger C, Wang L, Berner DK, Matschinsky FM (1996) Glucose metabolism and insulin release in mouse beta HC9 cells, as model for wild-type pancreatic beta-cells. Am J Physiol 270:E846–E857
6. Zhao C, Rutter GA (1998) Overexpression of lactate dehydrogenase A attenuates glucose-induced insulin secretion in stable MIN-6 beta-cell lines. FEBS Lett 430:213–216
7. Price NT, Jackson VN, Halestrap AP (1998) Cloning and sequencing of four new mammalian monocarboxylate transporter (MCT) homologues confirms the existence of a transporter family with an ancient past. Biochem J 329:321–328
8. Zhao C, Wilson MC, Schuit F, Halestrap AP, Rutter GA (2001) Expression and distribution of lactate/monocarboxylate transporter isoforms in pancreatic islets and the exocrine pancreas. Diabetes 50:361–366
9. Ishihara H, Wang H, Drewes LR, Wollheim CB (1999) Overexpression of monocarboxylate transporter and lactate dehydrogenase alters insulin secretory responses to pyruvate and lactate in beta cells. J Clin Invest 104:1621–1629
10. Meissner T, Otonkoski T, Feneberg R, Beinbrech B, Apostolidou S, Sipila I, Schaefer F, Mayatepek E (2001) Exercise induced hypoglycaemic hyperinsulinism. Arch Dis Child 84: 254–257
11. Otonkoski T, Kaminen N, Ustinov J, Lapatto R, Meissner T, Mayatepek E, Kere J, Sipila I (2003) Physical exercise-induced hyperinsulinemic hypoglycemia is an autosomal-dominant trait characterized by abnormal pyruvate-induced insulin release. Diabetes 52:199–204
12. Meissner T, Friedmann B, Okun JG, Schwab MA, Otonkoski T, Bauer T, Bartsch P, Mayatepek E (2005) Massive insulin secretion in response to anaerobic exercise in exercise-induced hyperinsulinism. Horm Metab Res 37:690–694
13. Kruglyak L, Daly MJ, Reeve-Daly MP, Lander ES (1996) Parametric and nonparametric linkage analysis: a unified multipoint approach. Am J Hum Genet 58:1347–1363
14. Staden R (1996) The Staden sequence analysis package. Mol Biotechnol 5:233–241
15. Van Lommel L, Janssens K, Tsukamoto K, Quintens R, Vander Mierde D, Lemaire K, Denef C, Martens G, Jonas J-C, Pipeleers D, et al (2006) Probe-independent and direct quantification of insulin mRNA and growth hormone mRNA in enriched cell preparations. Diabetes 55:3214–3220
16. Parton LE, Diraison F, Neill SE, Ghosh SK, Rubino MA, Bisi JE, Briscoe CP, Rutter GA (2004) Impact of PPARγ overexpression and activation on pancreatic islet gene expression profile analyzed with oligonucleotide microarrays. Am J Physiol Endocrinol Metab 287:E390–E404
17. Cuff MA, Shirazi-Beechey SP (2002) The human monocarboxylate transporter, MCT1: genomic organization and promoter analysis. Biochem Biophys Res Commun 292:1048–1056
18. Ullah MS, Davies AJ, Halestrap AP (2006) The plasma membrane lactate transporter MCT4, but not MCT1, is up-regulated by hypoxia through a HIF-1α-dependent mechanism. J Biol Chem 281:9030–9037
19. Sambrook J, Russell DW (2001) Gel retardation assays for DNA-binding proteins: molecular cloning. Cold Spring Harbor Laboratory Press, Cold Spring Harbor, New York, pp 17.13–17.17
20. Kirk P, Wilson MC, Heddle C, Brown MH, Barclay AN, Halestrap AP (2000) CD147 is tightly associated with lactate transporters MCT1 and MCT4 and facilitates their cell surface expression. EMBO J 19:3896–3904
21. Halestrap AP, Price NT (1999) The proton-linked monocarboxylate transporter (MCT) family: structure, function and regulation. Biochem J 343:281–299
22. Halestrap AP, Meredith D (2004) The SLC16 gene family—from monocarboxylate transporters (MCTs) to aromatic amino acid transporters and beyond. Pflugers Arch 447:619–628
23. Bryan J, Crane A, Vila-Carriles WH, Babenko AP, Aguilar-Bryan L (2005) Insulin secretagogues, sulfonylurea receptors and K(ATP) channels. Curr Pharm Des 11:2699–2716
24. Salt IP, Johnson G, Ashcroft SJ, Hardie DG (1998) AMP-activated protein kinase is activated by low glucose in cell lines derived from pancreatic beta cells, and may regulate insulin release. Biochem J 335:533–539